White Rose Research Online

eprints@whiterose.ac.uk
https://eprints.whiterose.ac.uk
Universities of Leeds, Sheffield and York

Deposited via The University of Sheffield.

White Rose Research Online URL for this paper:
https://eprints.whiterose.ac.uk/id/eprint/238607/

Version: Published Version

Article:
Parga, E.F.D., Wolverson, P.A., Collins, M.O. et al. (2026) Acetyl-phosphate dependent protein acetylation in Neisseria gonorrhoeae. Microbiologyopen, 15 (2). e70231. ISSN: 2045-8827

https://doi.org/10.1002/mbo3.70231

Reuse
This article is distributed under the terms of the Creative Commons Attribution (CC BY) licence. This licence allows you to distribute, remix, tweak, and build upon the work, even commercially, as long as you credit the authors for the original work. More information and the full terms of the licence here: https://creativecommons.org/licenses/

Takedown
If you consider content in White Rose Research Online to be in breach of UK law, please notify us by emailing eprints@whiterose.ac.uk including the URL of the record and the reason for the withdrawal request.

UNIVERSITY OF LEEDS
University of Sheffield
UNIVERSITY of York

Check for updates

MicrobiologyOpen

WILEY

MicrobiologyOpen Open Access

ORIGINAL ARTICLE OPEN ACCESS

Acetyl-Phosphate Dependent Protein Acetylation in *Neisseria gonorrhoeae*

Ernesto F. D. Parga[1,2] | Paige A. Wolverson[1,2,3] | Mark O. Collins[4] | Oliver Heaney[1,2] | Joby Cole[1,2] | Luke R. Green[2,3] | Jonathan G. Shaw[1,2]

[1]Division of Clinical Medicine, School of Medicine and Population Health, University of Sheffield, Sheffield, South Yorkshire, UK | [2]Florey Institute of Infection, University of Sheffield, Sheffield, South Yorkshire, UK | [3]School of Clinical Dentistry, University of Sheffield, Sheffield, South Yorkshire, UK | [4]School of Biosciences, University of Sheffield, Sheffield, South Yorkshire, UK

Correspondence: Luke R. Green (l.r.green@sheffield.ac.uk) | Jonathan G. Shaw (j.g.shaw@sheffield.ac.uk)

Received: 11 March 2025 | **Revised:** 23 January 2026 | **Accepted:** 28 January 2026

Funding: University of Sheffield; CONACyT

Keywords: acetate kinase | acetylome | acetyl-phosphate | *Neisseria gonorrhoeae* | phosphotransacetylase

ABSTRACT

The disease gonorrhoea is caused by the sexually transmitted pathogen *Neisseria gonorrhoeae*. This bacterium is an obligate human pathogen that can survive intracellularly through the expression of specific pathogenicity determinants. Protein post-translational modifications have been shown to be involved in the regulation of gene transcription and metabolism. Here, we studied the role of non-enzymatic acetylation by acetyl-phosphate in *N. gonorrhoeae*. This was achieved through the deletion of *pta* and *ackA* genes from the phosphotransacetylase-acetate kinase pathway (PTA-AKA) that modulate the level of acetyl-phosphate in the cell. As predicted, more protein acetylation was observed in the Δ*ackA* strain. Using immunoaffinity purification of acetylated peptides and LC-MS/MS we demonstrated that 88% of the detectable *N. gonorrhoeae* proteome (1343 proteins) is acetylated. With many of the acetylated proteins involved in central metabolism especially in pyruvate utilisation. Growth studies showed that the Δ*ackA* strain was unable to utilise pyruvate as a carbon source, whereas it could grow on glucose as well as the wild-type. Furthermore, a deacetylase enzyme was identified and its gene mutated (Δ*hdac*), this allowed the identification of a number of putative targets for HDAC, including phosphotransacetylase. We found that gonococcal pathogenicity was changed by acetyl-phosphate concentration, with the Δ*ackA* strain killing the wax moth larvae faster than the wild-type, whereas the Δ*pta* strain was non-pathogenic in this model. The data obtained suggest that non-enzymatic protein acetylation in *N. gonorrhoeae* plays an important role in the central metabolism, carbon source utilisation, and virulence of this bacterium.

1 | Introduction

Neisseria gonorrhoeae is one of the most common sexually transmitted bacteria in the United Kingdom and is the causative agent of gonorrhoea. In men, the disease presents as an acute urethritis, however, in women the infection is often asymptomatic but can give rise to Pelvic Inflammatory Disease (PID) leading to serious complications such as ectopic pregnancy, tubal infertility, and chronic pelvic pain. Gonorrhoeal infections are increasing worldwide, in England in 2022 there was an increase of 50.3% on the previous year (UK Health Security Agency 2023). Currently, we are experiencing the largest number of new gonorrhoea cases diagnosed since the 1970s (Public Health England 2018). Worldwide, there are thought to be 82.4 million new gonococcal infections per year (Unemo et al. 2019). Over time, *N. gonorrhoeae* has gained resistance to many of the antibiotics used for the treatment of gonococcal disease, and there has been an increase in the isolation of

This is an open access article under the terms of the Creative Commons Attribution License, which permits use, distribution and reproduction in any medium, provided the original work is properly cited.

© 2026 The Author(s). *MicrobiologyOpen* published by John Wiley & Sons Ltd.

multidrug-resistant strains. The current first-line treatment of gonococcal infection is the injectable cephalosporin, ceftriaxone (Fifer et al. 2020). However, resistance to ceftriaxone is increasing (Fifer et al. 2020). The World Health Organisation has highlighted the need for improved and continued antimicrobial resistance (AMR) surveillance for *N. gonorrhoeae*, describing it as a high-priority pathogen (Fifer et al. 2020).

Currently, there are no vaccines available for *N. gonorrhoeae*, therefore, improved therapy for gonococcal disease will require enhanced knowledge of the organisms physiology for the development and discovery of new therapeutics for its treatment. *N. gonorrhoeae* colonises and infects diverse sites within the human host, these represent unique niches with varying nutrients and environmental factors (Green et al. 2022). The pathogenic *Neisseria* are fastidious organisms that are only able to grow on glucose, lactate, and pyruvate as primary carbon sources. Our previous work on the virulence of the pathogenic *Neisseria* has shown the importance of lactate in pathogenicity and the significance of studying the physiology of these organisms (Exley, Goodwin, et al. 2005; Exley, Shaw, et al. 2005; Exley et al. 2007). Neisserial growth on lactate has been demonstrated to stimulate growth, with a more rapid emergence from lag-phase and increases in LOS-sialylation (Exley et al 2005; Parsons et al. 1996). Mutation of the neisserial lactate transporter, LctP, resulted in attenuation of the meningococcus in a rat septicaemia model and reduced colonization of human nasopharyngeal explants (Exley, Goodwin, et al. 2005; Exley, Shaw, et al. 2005). Whereas, an LctP mutation in *N. gonorrhoeae* caused a reduced colonisation of the murine genital tract (Exley et al. 2007). We have previously observed that neisserial utilisation of lactate results in the excretion of acetate from the bacterial cell, this can be seen both during growth in chemically defined media and in human cerebrospinal fluid (CSF) (Exley, Shaw, et al. 2005; Leighton et al. 2001).

Once transported into the neisserial cell, the lactate dehydrogenase (Ldh) enzymes convert lactate to pyruvate and then to acetyl-CoA by pyruvate dehydrogenase (Pdh). In *Neisseria*, much of the carbon flux from lactate is metabolised via acetyl-CoA and, rather than entering the TCA cycle, is consumed in a mixed acid fermentation step. This results in acetate excretion via an acetyl-phosphate intermediate with the production of ATP (Exley, Shaw, et al. 2005; Leighton et al. 2001). The two key enzymes in this pathway are phophotransacetylase (Pta) that converts acetyl-CoA to acetyl-phosphate and acetate kinase (AckA) that converts acetyl-phosphate to acetate with the release of ATP (Figure 1A). Previously, we observed in the pathogenic *Neisseria*, the specific activity of Pta is much higher than that of AckA (Leighton et al. 2001), suggesting an increase in the acetyl-phosphate pool of the cell. Acetyl-phosphate can act as a direct phosphoryl donor to two-component sensor-regulator systems (TCS) and therefore may be a modulator of gene expression (McCleary et al. 1993). However, acetyl-phosphate has been shown to have a global regulatory role by acting as a general acetyl donor in the non-enzymatic acetylation of Nε-lysines on proteins and thereby modulating their activity (Weinert et al. 2013; Wolfe 2016). In bacteria this non-enzymic acetyl-phosphate-dependent acetylation is specific, with only a number of specific lysines being acetylated, this process accounts for most of the global protein acetylation versus enzyme-dependent protein acetylation (Wolfe 2016).

Previously, Post and co-workers (2017) have demonstrated the presence of 2686 acetyl phosphate-dependent acetylation sites on the proteins of *N. gonorrhoeae* utilising an acetate kinase mutant (*ackA*). In this study we have utilised both gonococcal Δ*ackA* and Δ*pta* mutants to further investigate the neisserial acetylome, thereby improving the repertoire of gonococcal acetylated proteins. We have also identified a deacetylase enzyme HDAC and through an Δ*hdac* mutant identified its target proteins in *N. gonorrhoeae* acetylome. Furthermore, we have demonstrated for the first time a role for the PTA-AK pathway in gonococcal virulence utilising the *Galleria mellonella* infection model.

2 | Materials and Methods

2.1 | Bacterial Strains and Media

N. gonorrhoeae MS11 was the wild-type parental strain for the creation of mutants of the phosphotransacetylase acetate kinase (PTA-AK) pathway (Table 1). Stocks of *N. gonorrhoeae* MS11 were stored at −80°C and routinely grown on chocolate agar (CHO) or Gonococcus agar (GC) (Oxoid) with 1% Kellogg's supplements at 37°C and 5% CO_2 atmosphere. Mutant strains of the *N. gonorrhoeae* were grown on a GC agar with 80 μg/mL kanamycin under the same growth conditions. For liquid growth, brain heart infusion broth (Oxoid) supplemented with 0.5% yeast extract (Oxoid) (BHI-Y) and 10 mM $NaHCO_3$ was used. Broth cultures were incubated at 37°C with shaking at 120 rpm.

For carbon source utilisation, a chemically defined medium for *N. gonorrhoeae* (CDM-GC) was used (Morse and Bartenstein 1980).

2.2 | Construction and Characterisation of *ackA*, *hdac*, and *pta* Mutants

N. gonorrhoeae MS11 Δ*ackA* (NGFG00758, NGO0977, HT085_RS05270) and Δ*pta* (NGFG00350, NGO0214, HT085_RS01430) mutants were created as follows: genomic DNA (gDNA) was extracted from previously created *N. meningitidis* MC58 Δ*ackA*::*kan*^{r} and *N. meningitidis* MC58 Δ*pta*::*kan*^{r} mutants (Catenazzi et al. 2014). The meningococcal mutants had an internal part of the gene of interest deleted and a kanamycin resistance cartridge *(nptII)* inserted into the deletion. This kanamycin cartridge that contains an outward reading promoter that drives the transcription of downstream genes when inserted in the correct orientation to reduce polar effects. The mutant meningococcal gDNA was amplified by PCR with Q5 high-fidelity DNA Polymerase (New England Biolabs) and primers for *ackA*

(F 5′-TCCCAAAAATTGATCTTGG; R 5′-GTGGGCAATCATCA GCTCTT) and *pta* (F 5′-GTCGCCGCTTAAAAAGA; R 5′-ATT TCCGCCGTCCTCCAT).

The *hdac* gene (NGFG00325, NGO0187, HT085_RS01305) of the *N. gonorrhoeae* was mutated through the insertion of a kanamycin resistance gene (*kan*^{r}) by annealing PCR, inserting the resistance marker at the nucleotide position 468 using primers *hdac*1-F (5′-TGAAACTCTACGCCCTGTTG), *hadc*1-R (5′-*TCAT TTTAGCCAT*AACGTTGTTCAGCAG), *hdac*2-F (5′- *TGAATTGT TTTAG*TGTTTGAAACCGACCTTTT), and *hdac*2R (5′- TTCAG ACGGCATTTATATCG). The underlined sequence in italics

20458827, 2026, 2, Downloaded from https://onlinelibrary.wiley.com/doi/10.1002/mbo3.70231 by Open Access Sheffield - UNIVERSITY OF SHEFFIELD , Wiley Online Library on [03/03/2026]. See the Terms and Conditions (https://onlinelibrary.wiley.com/terms-and-conditions) on Wiley Online Library for rules of use; OA articles are governed by the applicable Creative Commons License

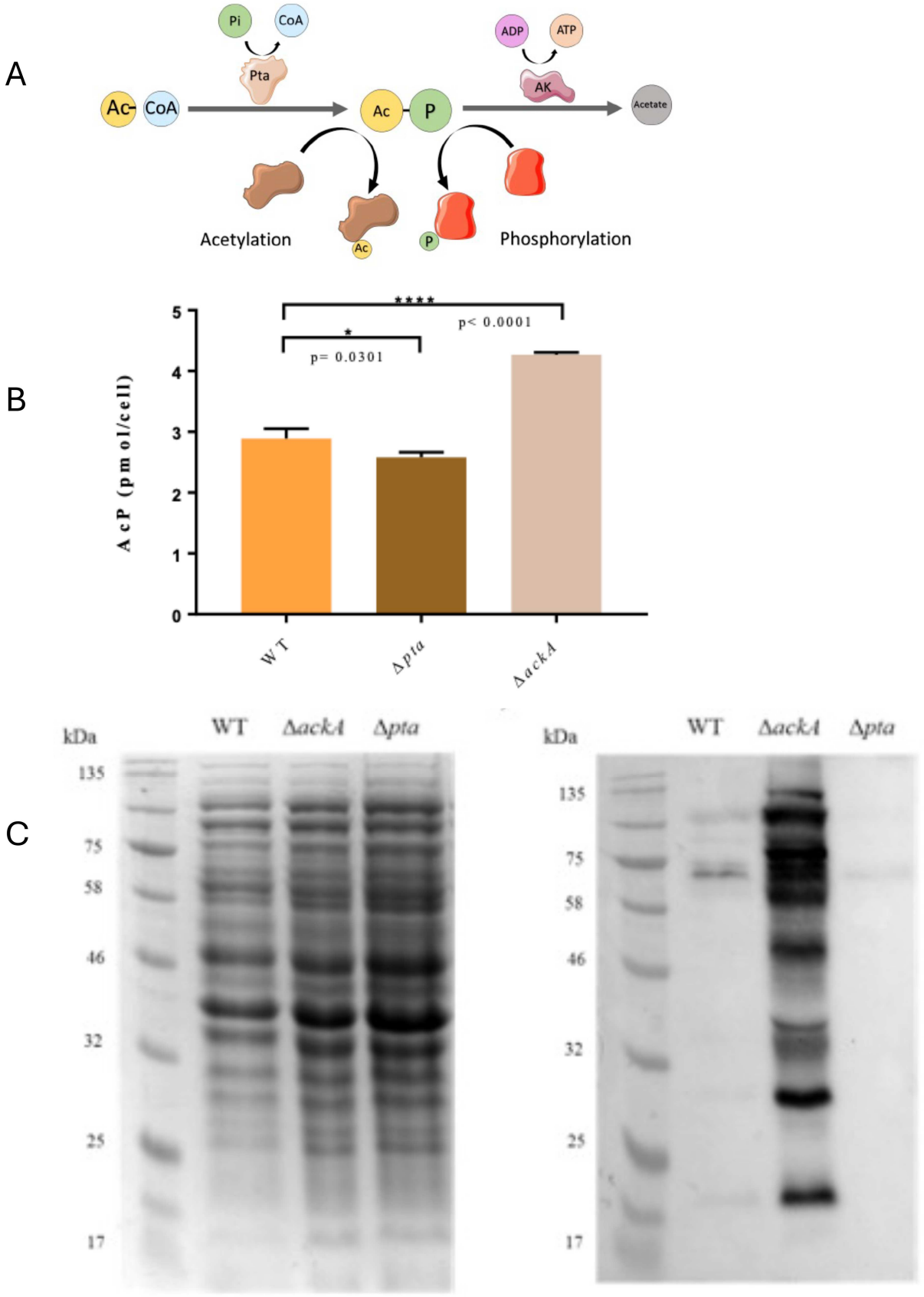

FIGURE 1 | Legend on next page.

20458827, 2026, 2, Downloaded from https://onlinelibrary.wiley.com/doi/10.1002/mbo3.70231 by Open Access Sheffield - UNIVERSITY OF SHEFFIELD , Wiley Online Library on [03/03/2026]. See the Terms and Conditions (https://onlinelibrary.wiley.com/terms-and-conditions) on Wiley Online Library for rules of use; OA articles are governed by the applicable Creative Commons License

TABLE 1 | Bacterial strains and constructs used in this study.

Strain	Description and genotype	Source
N. gonorrhoeae MS11	Wild type, isolated from uncomplicated gonorrhoea, contains gonococcal genetic island.	Swanson (1972)
N. gonorrhoeae MS11 Δ*ackA*::*kan*^{r}	MS11 with disrupted genomic copy of *ackA* by insertion of kanamycin resistance gene.	This study
N. gonorrhoeae MS11 Δ*pta*::*kan*^{r}	MS11 with disrupted genomic copy of *pta* by insertion of kanamycin resistance gene.	This study
N. gonorrhoeae MS11 Δ*hdac*::*kan*^{r}	MS11 with disrupted genomic copy of *hdac* by insertion of kanamycin resistance gene.	This study
Escherichia coli DH5α	F$^-$ *endA1 gln*V44 *thi-1 recA1 relA1 gyr*A96 *deoR nupG purB20* φ80d*lac*ZΔM15 Δ(*lacZYA-argF*)U169, hsdR17($r_k^-m_k^+$), λ$^-$	New England Biolabs

corresponds to the overlapping sequence between the *hdac* and the kanamycin resistance cassette amplified using primers kanF (5′-*CTGAACAACGTT*ATGGCTAAAATGAGAATATCAC) and kanR (5′ *TCGGTTTCAAACA*CTAAAACAATTCATCCAGT AAAA). To complete the DNA uptake sequence (DUS), one base pair was added to the *hdac*2-R primer.

Agar spot transformation was done as described by Dillard (2011). Overnight colonies of *N. gonorrhoeae* MS11 grown on chocolate agar were streaked on the dried DNA spots and incubated for 48 h. Then colonies grown on the spot were streaked on GC agar supplemented with 80 μg/mL kanamycin and incubated for selection. Sequencing was performed to confirm the mutant construction.

Several attempts were made to complement the mutations, however, all attempts were unsuccessful. A similar finding was also reported by Post and co-workers (2017), who were also unable to complement similar genes.

2.3 | Carbon Utilisation

The neisserial strains were grown in liquid cultures of CDM-GC supplemented with either 10 mM glucose or 20 mM lactate (Felix Diaz Parga 2021; Morse and Bartenstein 1980). Growth was measured by spectrophotometer at OD 600 nm. For initiation of the growth curves, the culture was adjusted to an OD_{600} of 0.05 and the change in absorbance measured over time as the tubes were incubated at 37°C with shaking at 120 rpm.

2.4 | Protein Electrophoresis and Western Blotting

Bacterial cell lysates were prepared from samples of MS11-derived strains that had been grown on different carbon sources. Protein concentrations of cell-free extracts were measured by BCA assay (Pierce) and analysed by western blot. Sample concentrations were normalised to 20 μg per lane and electrophoresed proteins were transferred to nitrocellulose and blocked in PBST (PBS with 0.1% Tween® 20 (v/v)) with 5% skimmed milk (w/v) for 1 h. The blot was incubated overnight at 4°C with the anti-acetyl-lysine polyclonal rabbit antibody (Cell Signaling Technology) diluted 1:1000 in PBST with 5% (w/v) skimmed milk followed by a horseradish peroxidase-conjugated goat anti-rabbit secondary antibody (Cell Signaling Technology) was diluted 1:5000 in PBST with 5% (w/v) skimmed milk at room temperature for 1 h. The blot was developed using a chemiluminescence substrate (ECL™ GE Healthcare Life Science).

2.5 | Acetyl-Phosphate (AcP) Quantification

The concentration of AcP in the bacterial cell was determined from the release of ATP following the conversion of AcP to acetate performed by acetate kinase (Weinert et al. 2013). Briefly, strains were grown for 10 h and extracted by the addition of 100 μL 3 M $HClO_4$ (perchloric acid). The bacterial suspension were centrifuged and neutralised with 100 μL saturated $KHCO_3$. Lysates were then filter sterilised. For AcP measurement the reaction mixture contained 50 μL lysate, 2 μL 100 mM $MgCl_2$, 4 μL 300 mM ADP, and 4 μL 0.4 U/μL acetate kinase. ATP was determined by mixing 50 μL of the reaction with 50 μL CellTiter-Glo® reagent (Promega, Madison, WI, USA).

2.6 | Cell Free Extract

Neisserial cultures were grown in CDM-GC supplemented with 10 mM glucose for 7 h. The bacteria were centrifuged

FIGURE 1 | PTA-AK pathway controls the concentration of acetyl-phosphate. (A) The phosphotransacetylase acetate kinase pathway, showing acetyl-phosphate (AcP) as an intermediate. AcP can be used as an acetyl group donor for the acetylation of proteins, or a phosphate donor to sensor kinase proteins of two-component systems (TCS). (B) The AcP concentration was quantified from cell-free extracts obtained from each strain of *Neisseria gonorrhoeae* MS11 grown on BHI broth for 10 h. A standard curve of AcP was used to calculate the concentration of AcP in pmoles per cell. The number of cells was measured by the OD_{600} of the WT, Δ*pta*, and Δ*ackA* strains with values of 0.332, 0.170, and 0.244, respectively. Measurements were performed by triplicate. Δ*ackA* strain showed a significant higher concentration of AcP and Δ*pta* a significant lower concentration, both compared to the WT, with biological replicates $n = 3$. (C) SDS-PAGE loading control and representative image of an immunoblot for acetylated proteins using an anti-acetyllysine antibody. Strains of *N. gonorrhoeae* MS11 were grown in BHI-Y for 24 h.

20458827, 2026, 2, Downloaded from https://onlinelibrary.wiley.com/doi/10.1002/mbo3.70231 by Open Access Sheffield - UNIVERSITY OF SHEFFIELD, Wiley Online Library on [03/03/2026]. See the Terms and Conditions (https://onlinelibrary.wiley.com/terms-and-conditions) on Wiley Online Library for rules of use; OA articles are governed by the applicable Creative Commons License

and the pellet was re-suspended with 2.5 mL denaturation buffer and sonicated on ice 10 times at ~20 A for 30 s. Protein concentrations were quantified using the Pierce BCA protein assay kit.

2.7 | LC-MS/MS Sample Preparation

N. gonorrhoeae strains were grown in CDM-GC and cell-free extracts (CFE) created. The cell-free extract samples were reduced in 10 mM tris-2(-carboxyethyl)-phosphine (TCEP) and in alkylated in 20 mM iodoacetamide in darkness. Samples were diluted in 50 mM ammonium bicarbonate and digested with trypsin-TPCK (Cell Signaling Technology). The samples were then acidified with TFA (trifluoroacetic acid). Sep-Pak C18 columns (Waters) were washed with 100% acetonitrile (ACN) followed by 50% ACN and then 0.1% TFA. The Sep-Pak C18 column was equilibrated with 0.1% TFA. Cell-free extract samples were added to the column and washed with 0.1% TFA, samples were eluted with 50% ACN. Peptide samples were dried in a SpeedVac concentrator and re-suspended in immunoaffinity purification buffer (Cell Signalling Technology). Anti-acetyl-lysine antibodies coupled to beads were used to immunoaffinity purify any acetylated peptides according to the manufacturer's instructions (Cell Signalling Technology). Eluted peptides from the immunoaffinity purifications were desalted and washed with 0.1% TFA/50% ACN followed by 0.1% TFA. Subsequently, followed by 3 more washes with 0.1% TFA, peptides were eluted with TFA/50% ACN. Finally, the peptides were vacuum-dried and dissolved in 0.5% formic acid.

2.8 | Mass Spectrometry Analysis

The peptide samples were investigated by nanoflow LC-MS/MS using the methodology previously described (English et al. 2024).

2.9 | Mass Spectrometry Data Analysis

Raw mass spectrometry data were analysed as described before (English et al. 2024) using MaxQuant version 1.6.5 against a *N. gonorrhoeae* UniProt reference. Data from mass spectrometry were deposited in the PRIDE partner repository via the ProteomeXchange Consortium with the dataset identifier (PXD060162).

2.10 | Motif Analysis, Enrichment Analysis, and Network Interactions

Potential motifs for acetylation were investigated 5 amino acids upstream and downstream of the site of acetylation and for analysis of enrichment using the DAVID Bioinformatic Resource 6.7 (Huang et al. 2007), using the settings of Yu et al. (2008). A corrected $p < 0.05$ was considered significant for all the enrichment analyses. For networks, the *enrichplot* package was used.

2.11 | *G. mellonella* Infection Assay

A modified protocol of larvae killing assay of Wand et al. (2011) was used to determine if *N. gonorrhoeae* was able to infect wax moth larvae. The *N. gonorrhoeae* WT was grown to mid-log phase before centrifugation and resuspension in sterile PBS. Bacterial suspensions were adjusted to approximately 4×10^8 CFU/mL. Then serial dilutions in PBS were prepared. 10 μL bacterial suspension dilutions (10^2, 10^3, 10^4, 10^5, 10^6, 10^7, 10^8) were injected into the haemocoel via the hindmost left proleg of the larva. Groups of 20 larvae were used for each neisserial strain as well as control groups that were injected with 10 μL of PBS or 10 μL of heat-killed bacteria. The different larval infection groups were incubated separately at 37°C in a CO_2 incubator and monitored every 6 h for larval death.

2.12 | Nanopore Sequencing

Wild-type and *N. gonorrhoeae* Δ*pta*::*kan*^{r} and Δ*ackA*::*kan*^{r} mutants were confirmed and analysed using long-read Nanopore sequencing. Oxford Nanopore Technologies (ONT) Native Barcoding Kit 96 V14 (SQK-LSK114.96) was used to prepare the three DNA libraries and a blank negative control as per manfacturer's protocols. Libraries were loaded on to R10.4.1 flow cells and sequenced for 24 h on the ONT GridION. Trace files were basecalled using ONT Dorado (version 7.11.2) and high-accuracy basecalling settings. The resulting reads were assembled using Flye with three polish steps (version 2.9.6) and annotated using Prokka (version 1.14.6). Alignments of pilE were carried out using Clustal Omega.

2.13 | Infection Assays

Infection assays were performed as previously described (Green et al. 2023). Briefly, HEC-1B human endometrial cells were grown in MEM supplemented with 10% fetal calf serum (FCS). Approximately 1.5×10^5 cells were placed onto glass coverslips in 24-well plates and grown overnight. The bacterial WT or mutant strains at a multiplicity of infection (MOI) of 50 were used to infect the host cells for 1 h. Infected cells were fixed, washed, and stained with Giemsa stain before mounting and counting by light microscopy. Fields of view were chosen at random to enumerate a hundred cells and scored for the number of infected cells and infecting organisms.

2.14 | Statistics

Statistical analysis was performed using GraphPad Prism version 10.2.2 (GraphPad Software Inc., USA). All data represents at least three independent experiments and significance was established at $p \leq 0.05$. Statistical considerations and specific analyses are described separately within each section. * specify significance to the untreated control unless otherwise specified; *$p \leq 0.05$, **$p \leq 0.01$, ***$p \leq 0.001$.

3 | Results

To investigate acetyl-phosphate in non-enzymatic neisserial protein acetylation, the phosphotransacetylase-acetate kinase

20458827, 2026, 2, Downloaded from https://onlinelibrary.wiley.com/doi/10.1002/mbo3.70231 by Open Access Sheffield - UNIVERSITY OF SHEFFIELD , Wiley Online Library on [03/03/2026]. See the Terms and Conditions (https://onlinelibrary.wiley.com/terms-and-conditions) on Wiley Online Library for rules of use; OA articles are governed by the applicable Creative Commons License

(PTA-AK) pathway (Figure 1A) was interrupted by construction of isogenic mutants, *N. gonorrhoeae* Δ*pta*::*kan*^{r} and Δ*ackA*::*kan*^{r}, one predicted to lower the acetyl-phosphate concentration and the other to increase it, respectively (Verdin and Ott 2013). These mutations do not have polar effects as the cellular protein levels encoded by the genes immediately downstream of these mutations (*hisH* and *dsbD*) are not significantly different to those of the wild-type (Supporting table 1) and the whole-genome sequencing demonstrated no differences in flanking genes or intergenic regions.

The *pta* gene (NGFG00350, NGO0214) encodes a protein that produces acetyl-phosphate from acetyl-CoA. Mutation of *pta* inhibits production of acetyl-phosphate resulting in a decrease in the intracellular concentration. Whereas the mutant Δ*ackA* (NGFG00758, NGO0977) that encodes the enzyme that utilises acetyl-phosphate and produces acetate, this mutation causes an increase of the intracellular acetyl-phosphate concentration (Figure 1A).

The enzymatic activity of phosphotransacetylase (Pta) and acetate kinase (AckA), and the determination of the intracellular concentration of acetyl-phosphate (AcP) was done as an initial characterisation. This was to show that deletion of the *pta* and *ackA* genes gave the expected biological effect on the enzymatic activity and acetyl-phosphate concentration. When the genes were deleted the respective strains showed no enzymatic activity (Table 2). However, the AckA activity of the Δ*pta* mutant decreased by 45% in comparison with the WT, while the Pta activity of the Δ*ackA* mutant was reduced by 78% in relation to the WT strain (Table 2). As the activity of the enzymes was null in the respective mutants, a change in AcP production was expected so the intracellular concentration of AcP was quantified for the WT and Δ*pta* and Δ*ackA* mutants. As expected, a significant reduction in the intracellular concentration of AcP was seen in the Δ*pta* mutant compared to the WT strain, but a significant increase was seen in the Δ*ackA* mutant (Figure 1B).

As the two mutant strains showed differences in their AcP concentration a western blot using anti-acetyllysine antibody was performed. A different pattern of protein acetylation was expected as AcP is involved in the non-enzymatic protein acetylation (Klein et al. 2007; Wolfe 2016). A 12% acrylamide gel was loaded with 20 μg of cell-free extract per lane from the wild-type and mutant strains and transferred to nitrocellulose and immunoblotted for the presence of acetylated proteins (Figure 1C). The blot showed that the Δ*ackA* mutant had a greater intensity of acetylated bands compared to the WT, whereas the Δ*pta* mutant showed a lower band intensity (Figure 1C) demonstrating that these mutants provide the expected acetylation pattern.

3.1 | Acetylome of *N. gonorrhoeae* MS11 Wild-Type Strain

After demonstrating that *N. gonorrhoeae* undergoes AcP-dependent protein acetylation, the acetylome and proteome of the wild-type strain MS11 was characterised using quantitative mass spectrometry (MS). LC-MS/MS analysis of cell-free extracts identified 1249 proteins at a 1% FDR (Table S1). Immunoaffinity enrichment of acetylated peptides from the same digested cell-free extracts was performed and LC-MS/MS analysis identified 4245 class I acetylation sites in 1088 proteins (Table S2) which is the most comprehensive *N. gonorrhoeae* acetylome generated to date (Table S3). Class I acetylation sites were defined by a localisation probability of 0.75 and a probability localisation score difference greater than or equal to 5 as defined by Olsen et al. 2006). In total, 1343 proteins were identified from the proteome and acetylome profiling data combined, representing 63.6% coverage of the *N. gonorrhoeae* proteome, of which 81% was acetylated (Figure 2).

Acetylated proteins were analysed using the DAVID bioinformatics tool to determine cellular localisation and associated processes of the proteins. Analysis of the enrichment showed that the post-translational modification (PTM) acetylation was prevalent in a number of metabolic processes (Figure S1). The most significantly enriched proteins were in 55 biological processes. Metabolic processes were associated with the highest number of acetylated proteins (503 proteins) but the specific areas with the highest enrichment scores were in translation (80 proteins) and metabolic processes related to pyruvate (18), pyrimidines (16), and aspartic acid (18). 39 molecular function annotation terms were enriched with 28 of them related to binding, the highest was associated with rRNA binding. 17 terms were enriched for cellular components with the three highest enrichment scores associated with the ribosome containing more than 50 proteins each (Figure S1).

3.2 | Quantitative Analysis of Acetylome Changes in *ackA*, *pta*, and *hdac* Mutant Strains

The *N. gonorrhoeae* MS11 WT, Δ*ackA,* and Δ*pta* mutant strains were used to identify acetyl-phosphate-dependent acetylation sites. The potential deacetylase encoded by *hdac* (NGFG00325, NGO0187) was mutated to determine the sites of deacetylation on gonococcal proteins (Zughaier et al. 2020). The *N. gonorrhoeae*, WT, Δ*ackA*, Δ*hdac,* and Δ*pta*, were grown until mid-logarithmic phase was reached in CDM-GC supplemented with 10 mM glucose. Before 4 independent CFEs for each strain were enriched with the anti-acetyl-lysine antibody, the proteome of the samples were analysed to determine protein abundance changes (Table S1). The 16 replicates were evaluated by a Pearson correlation analysis and all samples had a correlation

TABLE 2 | Pta and AckA activity of *Neisseria gonorrhoeae* WT, Δ*pta,* and Δ*ackA*.

Strain	Pta ($nmol^{-1}min^{-1}mg^{-1}$)	AckA ($nmol^{-1}min^{-1}mg^{-1}$)
MS11 WT	1789.43 ± 267.38	9.78 ± 5.64
Δ*pta*	0	5.41 ± 3.86
Δ*ackA*	396.56 ± 87.94	0

Note: $n = 3$.

20458827, 2026, 2, Downloaded from https://onlinelibrary.wiley.com/doi/10.1002/mbo3.70231 by Open Access Sheffield - UNIVERSITY OF SHEFFIELD , Wiley Online Library on [03/03/2026]. See the Terms and Conditions (https://onlinelibrary.wiley.com/terms-and-conditions) on Wiley Online Library for rules of use; OA articles are governed by the applicable Creative Commons License

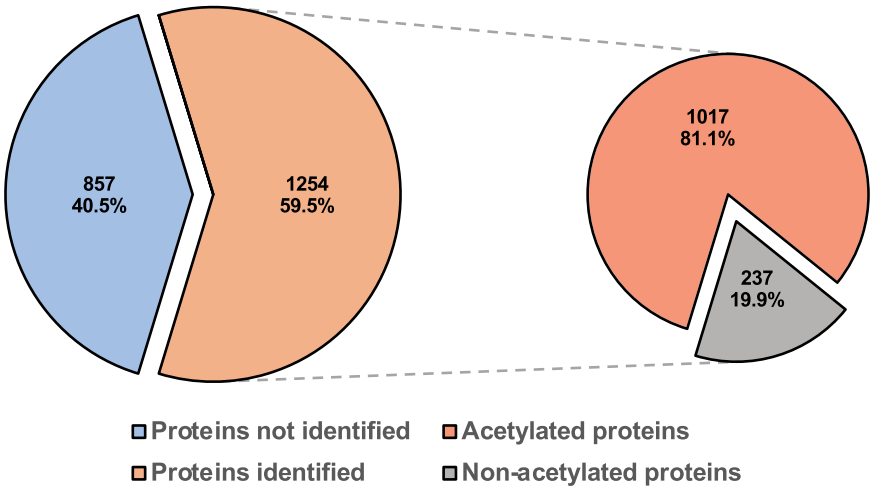

FIGURE 2 | Number of identified proteins of *Neisseria gonorrhoeae* MS11 by mass spectrometry. Total proteins identified by LC-MS/MS from *N. gonorrhoeae* MS11 proteome versus proteins identified after enrichment with the anti-acetyl lysine antibody (acetylome). 1343 proteins were identified from the proteome and acetylome profiling data combined, of which 81% (1088) of proteins identified were acetylated. 4245 class I acetylation sites in 1088 proteins were identified at a 1% false discovery rate.

value greater than 0.75 (Figure S2). Filtering of the data for site quantification based on a minimum of 3 biological replicates per group resulted in the identification of 3752 class I acetylation sites across 1017 proteins.

Statistical analysis of the quantitative differences in acetylation in *ΔackA, Δpta,* and Δ*hdac* mutant strains compared to WT was performed and large differences were observed (Table S2 and Figure 3A). To rule out that these differences were due to differential abundance of acetylated proteins, the same statistical analysis was performed on proteome profiling data obtained from the same set of samples and minimal overlap was found. Only 1.3% of significant altered acetylation sites between the mutant strains and WT mapped to proteins with significantly altered protein abundance (Tables S1 and S2).

Acetylation sites dependent on AcP that were determined as unique were found in both Δ*ackA* and Δ*pta*. These sites showed a significant ($p < 0.05$) increase or decrease of fold change, respectively, in at least three of the four biological replicates. The mean fold change in protein acetylation sites was 2.02 and −2.23 in Δ*ackA* and Δ*pta*, respectively and 409 acetylated proteins and 424 acetylation sites were identified (Figure 3B). Acetyl-phosphate-dependent acetylation sites were determined by analysing the increase and decrease from acetylation sites from the Δ*ackA* and Δ*pta* mutants, respectively. 117 unique acetylation sites were found in 102 proteins (Figure 3B) where 88 proteins showed one acetyl-phosphate-dependent acetylation site and 14 two sites.

Gene ontology analysis determined the term with the highest number of proteins with acetyl-phosphate dependent sites was ATP binding (38 proteins). KEGG pathway analysis showed pyruvate metabolism and methane metabolism with the highest number of acetylated proteins with 7 each. Glycolysis and gluconeogenesis had five acetylated proteins each. Most acetylated proteins were found in the cytoplasm (34) while 11 were integral membrane components (Figure 4). Translation had more than 5 proteins acetylated.

An enrichment analysis of AcP-dependent sites was performed, the highest enrichment score was related to tRNA aminoacylation and the other highest score was in metabolic processes. Most molecular function (65%) were related to binding (Figure 4).

3.3 | Determination of Targets for the Gonococcal Histone Deacetylase-Like Protein

HDAC are Histone deacetylase-like proteins, a family of enzymes that remove the acetyl group from the N-ε-lysine residue and were first discovered in eukaryotic cells (Grabiec and Potempa 2018). Recently, several HDAC-like proteins have been found in bacteria and that the gonococcal HDAC NGO0187 plays a role in the regulation of host gene expression (Jiang et al. 2017; Zughaier et al. 2020). To identify the possible targets of the gonococcal HDAC (NGO0187), the *hdac* gene was mutated and all the acetylation sites with a significant fold change from the WT were classified.

The role of HDAC is to deacetylate proteins, therefore, the possible targets for this enzyme were classified acetylation sites that showed a significant increase in the Δ*hdac* mutant strain. Thirty-four proteins with 34 unique acetylation sites were identified with this criterion (Figure 5). Three of these were tRNA ligases involved in translation and both ribosomal large subunits (50S and 30S) showed one target site each. Moreover, phosphotransacetylase (Pta) showed higher acetylation of K450, as well as PorB, a protein involved in the pathogenicity of *N. gonorrhoeae*, also showed one site.

Gene ontology analysis showed a diversity of functions; with the term translation as the only biological process with two proteins the others only one (Figure 5). ATP binding with 11 proteins followed by zinc ion binding, tRNA binding and magnesium ion binding were the highest molecular functions. While the metabolism of purine and pyrimidine showed 3 proteins. Enrichment analysis of the molecular functions demonstrated that all were binding related with the exception ATPase activity. tRNA binding had the highest enrichment score, with most proteins found in the cytoplasm (Figure 5).

20458827, 2026, 2, Downloaded from https://onlinelibrary.wiley.com/doi/10.1002/mbo3.70231 by Open Access Sheffield - UNIVERSITY OF SHEFFIELD , Wiley Online Library on [03/03/2026]. See the Terms and Conditions (https://onlinelibrary.wiley.com/terms-and-conditions) on Wiley Online Library for rules of use; OA articles are governed by the applicable Creative Commons License

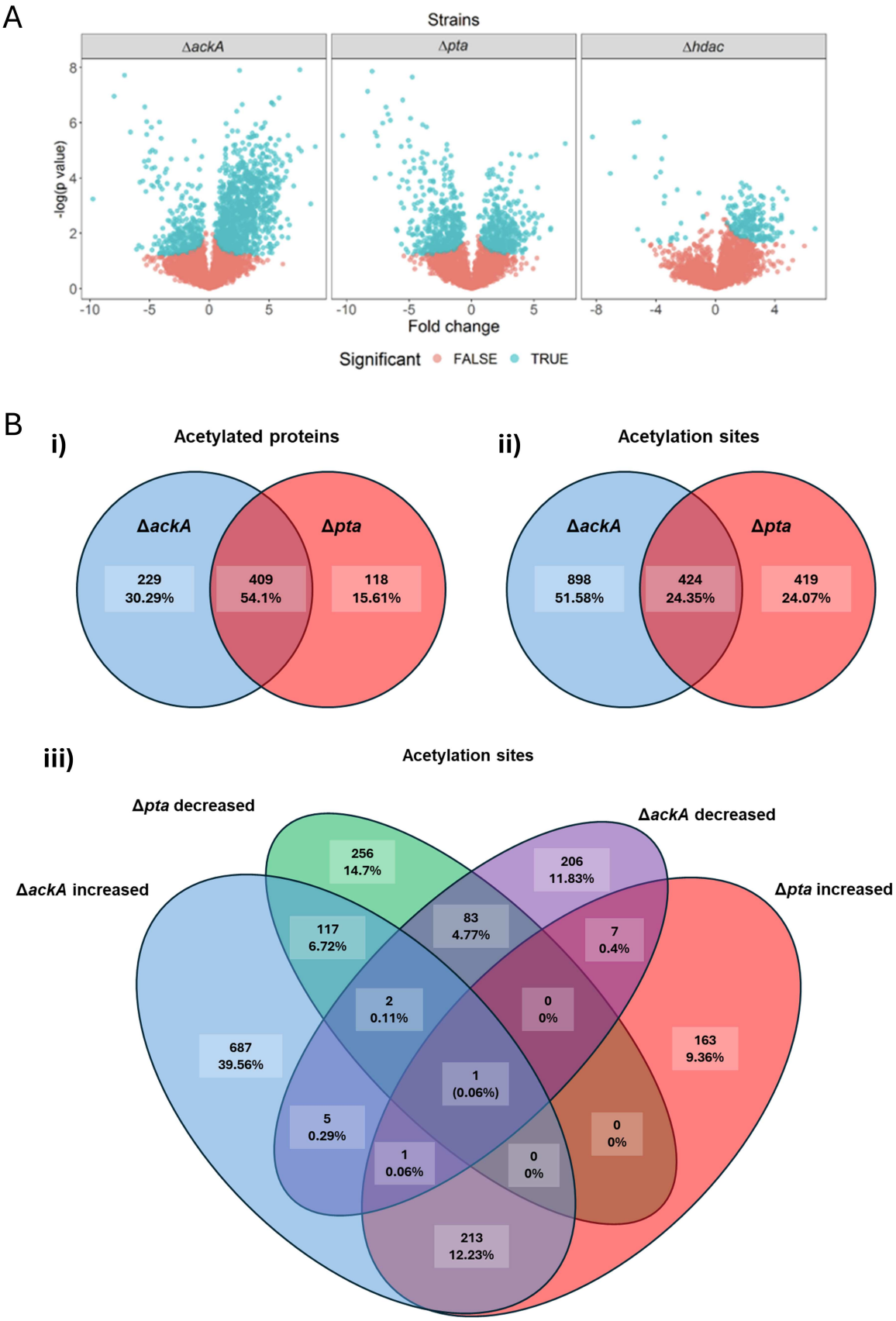

FIGURE 3 | Legend on next page.

20458827, 2026, 2, Downloaded from https://onlinelibrary.wiley.com/doi/10.1002/mbo3.70231 by Open Access Sheffield - UNIVERSITY OF SHEFFIELD , Wiley Online Library on [03/03/2026]. See the Terms and Conditions (https://onlinelibrary.wiley.com/terms-and-conditions) on Wiley Online Library for rules of use; OA articles are governed by the applicable Creative Commons License

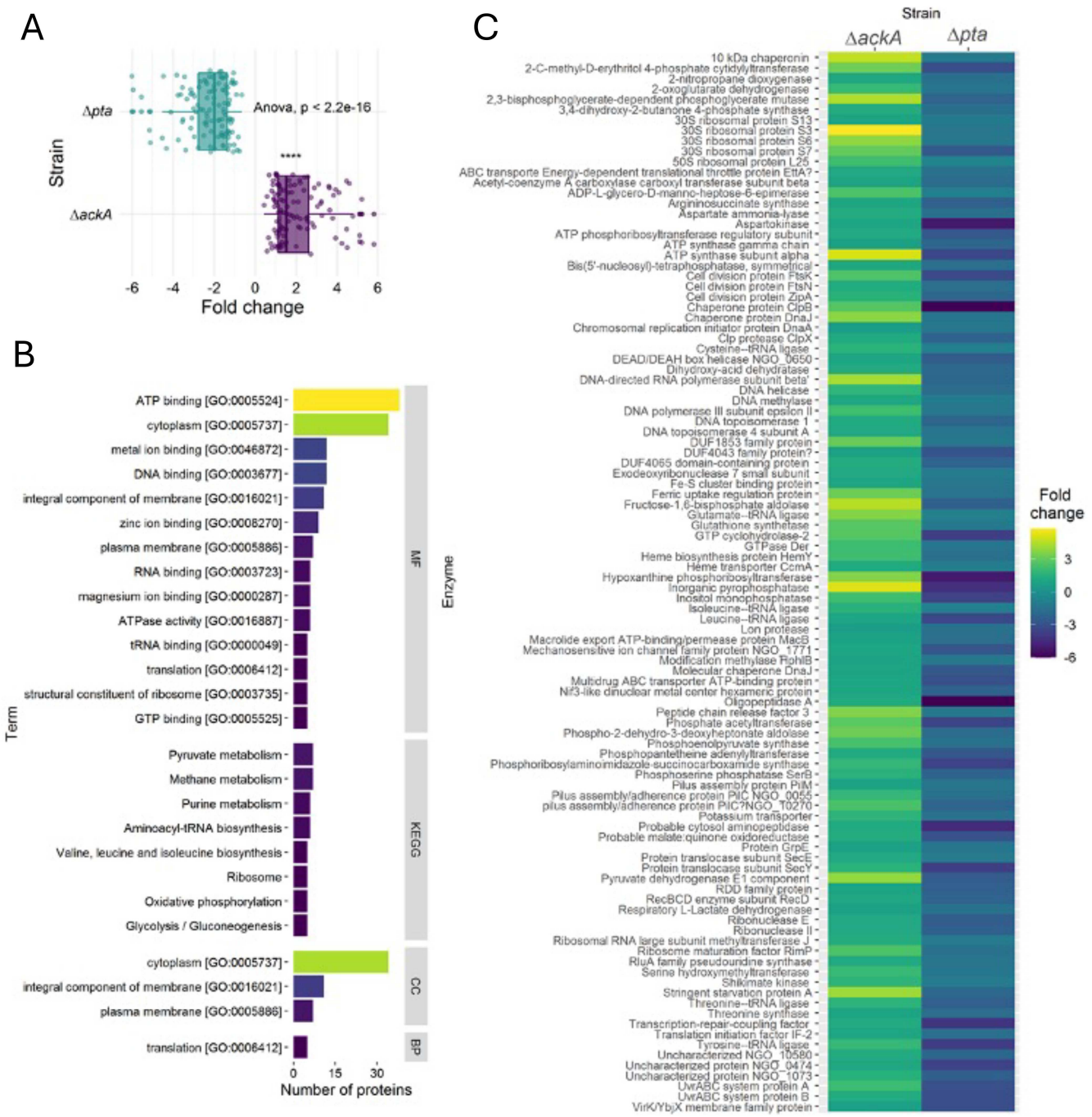

FIGURE 4 | Acetyl-phosphate-dependent sites. (A) Boxplot showing the fold change of each acetylation site. An ANOVA test shows a significant difference between the fold changes in both strains. (B) Gene ontology analysis showing the terms with more than five proteins in molecular function (MF), KEGG pathways (KEGG), cellular component (CC), and biological process (BP). (C) Proteins classified as acetyl-phosphate dependent for acetylation. The same acetylation site was found on both strains with a significant difference of the fold change. ANOVA, analysis of variance.

FIGURE 3 | Volcano plot for acetylation sites and Identification of unique acetyl-phosphate-dependent acetylation sites in *Neisseria gonorrhoeae* MS11. (A) The plot shows the acetylation sites that are significantly decreased (left side) or increased (right side), of the various mutants Δ*ackA*, Δ*pta,* and Δ*hdac* compared individually to the WT strain determined by the two-tailed Student's test. The S0 parameter was set to 0.1 and the false discovery rate to 0.05. Acetylation sites that showed a significant difference are blue coloured while the red are non-significant $n = 4$. (B) Venn diagrams of proteins and acetylation sites from the strains Δ*ackA* and Δ*pta*. (i) 409 unique proteins were shared between both strains, and (ii) 424 acetylation. (iii) Acetylation sites were divided into increased and decreased depending on the fold difference. The overlapping acetylation sites from Δ*ackA* with an increased fold difference and the decreased from Δ*pta* are the highly regulated acetyl-phosphate-dependent sites. A total of 117 unique acetylation sites were found in 102 proteins.

20458827, 2026, 2, Downloaded from https://onlinelibrary.wiley.com/doi/10.1002/mbo3.70231 by Open Access Sheffield - UNIVERSITY OF SHEFFIELD , Wiley Online Library on [03/03/2026]. See the Terms and Conditions (https://onlinelibrary.wiley.com/terms-and-conditions) on Wiley Online Library for rules of use; OA articles are governed by the applicable Creative Commons License

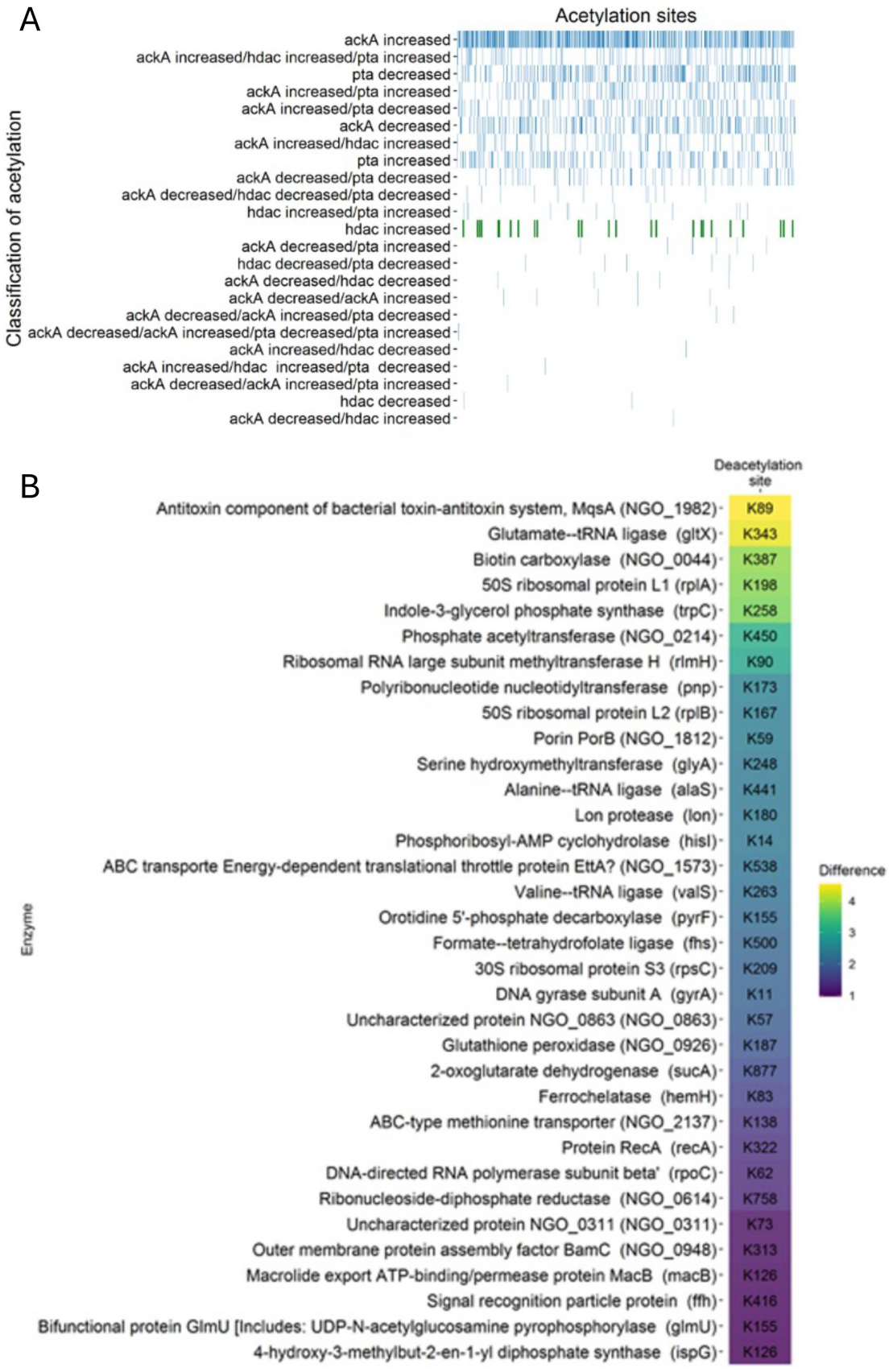

FIGURE 5 | Identification of the possible targets of HDAC. (A) The acetylation sites found in the three isogenic mutant strains Δ*ackA*, Δ*pta*, and Δ*hdac* were classified according to the fold change difference. From the 2451 acetylation sites (blue), 34 (green) were unique for Δ*hdac*. (B) List of the possible deacetylation sites of the protein HDAC in *Neisseria gonorrhoeae* MS11. The list shows the protein name and the gene name. The tiles are filled according the fold change difference and the deacetylation position site is found inside of the tile.

20458827, 2026, 2, Downloaded from https://onlinelibrary.wiley.com/doi/10.1002/mbo3.70231 by Open Access Sheffield - UNIVERSITY OF SHEFFIELD , Wiley Online Library on [03/03/2026]. See the Terms and Conditions (https://onlinelibrary.wiley.com/terms-and-conditions) on Wiley Online Library for rules of use; OA articles are governed by the applicable Creative Commons License

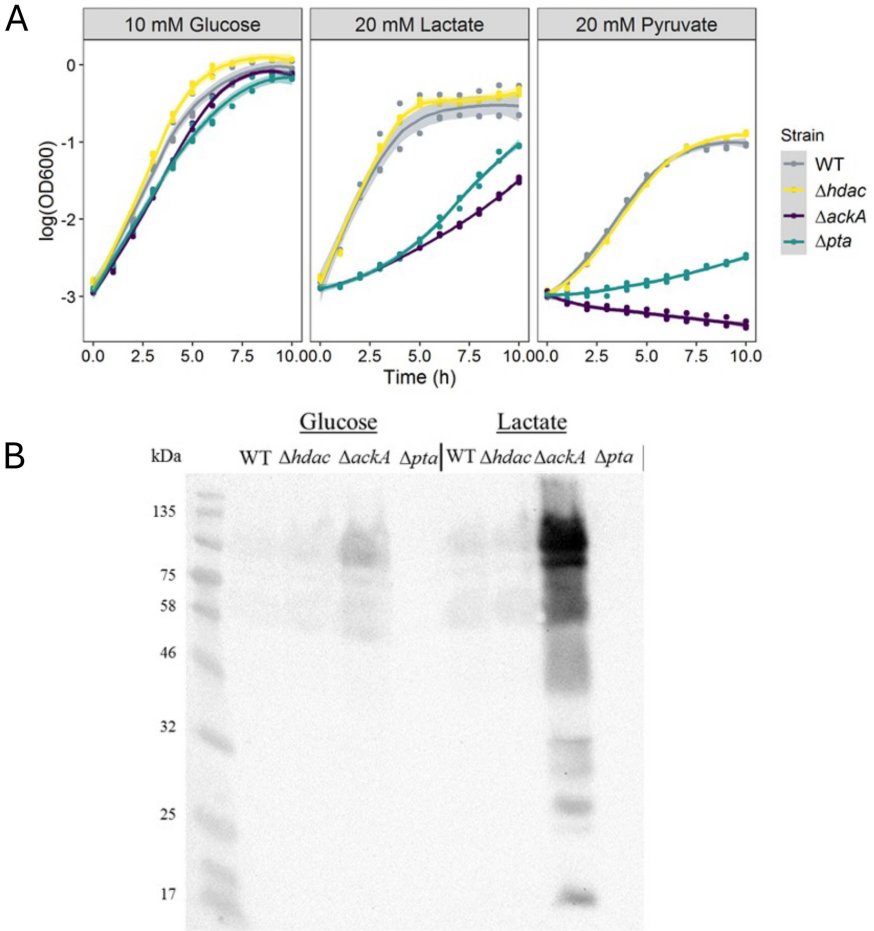

FIGURE 6 | Growth curves of *Neisseria gonorrhoeae* MS11 strains in glucose, lactate, and pyruvate and acetylation of proteins in *N. gonorrhoeae* MS11 in different carbon sources. Strains of *N. gonorrhoeae* MS11 were grown for 10 h at 37°C with shaking in a chemically defined medium supplemented with a carbon source. Samples were taken every hour and read in a spectrophotometer. (A) Growth curves of the 4 strains growing on the three different carbon sources. The plot shows the standard deviation of the curves. Samples of bacteria growing at 37°C in a chemically defined medium supplemented with 10 mM glucose or 20 mM lactate was taken for protein extraction. (B) 100 μg of proteins was loaded on a SDS-PAGE for western blot using an anti-acetyllysine antibody to detect acetylated proteins.

3.4 | The Δ*ackA* and Δ*pta* Mutants Affect the Ability to Utilise Different Carbon Sources

Investigation of the acetylome demonstrated changes in the acetylation state of many of the enzymes involved in the central metabolic processes of *N. gonorrhoeae*. Therefore, the ability of the WT and mutant strains to grow in chemically defined media with different primary carbon sources was investigated. All strains were able to grow on glucose as a primary carbon source, resulting in similar doubling times and yields (Figure 6A). When lactate was used as primary carbon sources, both the WT and Δ*hdac* mutant strain had similar growth rates and yields whereas the Δ*ackA* and Δ*pta* strain grew much more slowly (Figure 6A). This reduction in growth rate was more obvious when grown on pyruvate as the primary carbon source, the Δ*pta* strain had a much more restricted growth rate and the Δ*ackA* strain was unable to grow on this carbon source at all (Figure 6A). Whereas the wild-type and Δ*hdac* grew equally as well on pyruvate.

Previously, we have shown when the pathogenic *Neisseria* are grown on lactate they seem to prefer to utilise the PTA-AK pathway, as the specific activity of both of these enzymes is higher than when grown on glucose and more acetate, the end product of this pathway, is secreted into the media (Leighton et al. 2001; Exley, Shaw, et al. 2005). Therefore, we investigated the acetylation of proteins of the WT and mutants when grown on either glucose or lactate as the primary carbon source. Most protein acetylation was seen in the Δ*ackA* mutant strain when grown on both carbon sources (Figure 6B). However, the acetylated protein bands were much more intense when grown on lactate compared to those grown in glucose.

3.5 | The Δ*ackA* and Δ*pta* Mutants Affect Adherence and Survival in *Galleria*

Previous work has suggested a potential role for the PTA-AK pathway and AcP in neisserial pathogenesis (Zughaier et al. 2020; Exley et al. 2007). Therefore, the proteome of the Δ*ackA* and Δ*pta* mutants were investigated and compared to the wild-type *N. gonorrhoeae* MS11 as shown in the volcano plot (Figure 7).

We observed that proteins involved in type IV pili synthesis or pilus components were expressed significantly differently in the Δ*ackA* and Δ*pta* strains. The Δ*ackA* strain showed a significant increase of the pilin protein (NGO_11165), whereas, the Δ*pta*

20458827, 2026, 2, Downloaded from https://onlinelibrary.wiley.com/doi/10.1002/mbo3.70231 by Open Access Sheffield - UNIVERSITY OF SHEFFIELD , Wiley Online Library on [03/03/2026]. See the Terms and Conditions (https://onlinelibrary.wiley.com/terms-and-conditions) on Wiley Online Library for rules of use; OA articles are governed by the applicable Creative Commons License

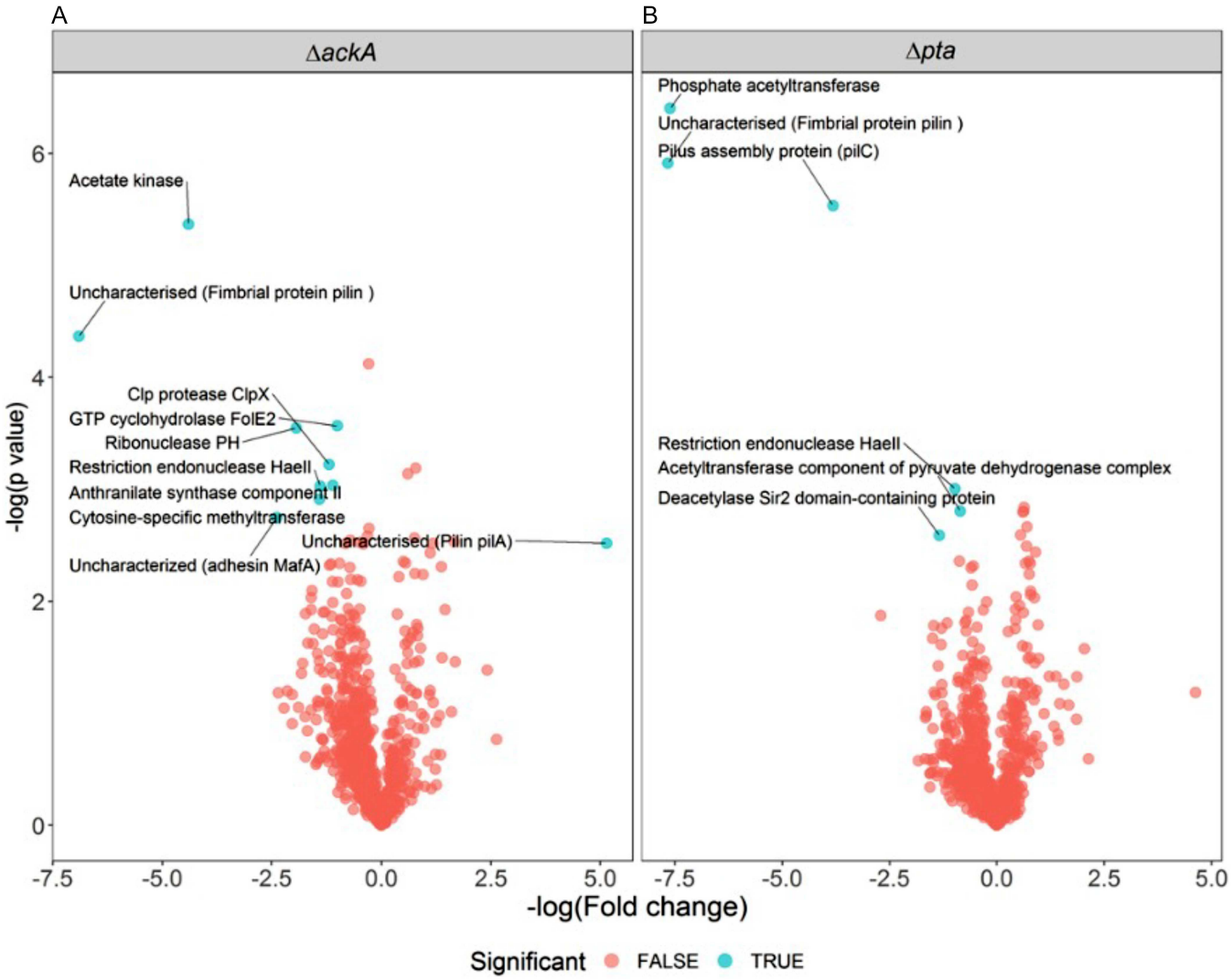

FIGURE 7 | Volcano plot of the proteome of *Neisseria gonorrhoeae*. (A) Protein extracts of the isogenic strains were analysed by mass spectrometry and the expression was analysed. In red and blue are the non-significant and significant different proteins for the isogenic strains Δ*ackA* and Δ*pta*. The significant different proteins are labelled with the name and abbreviation. (B) Significant different expressed proteins identified from mass spectrometry. The gene name or locus is shown next to the protein name. Experiment with 4 biological replicates.

strain demonstrated a significant decrease of the pilus assembly protein PilC (NGO_0055). The protein fimbrial protein pilin PilS2c1 (NGO_10980) decreased in both strains (Figure 7). Furthermore, a significantly lower expression of the MafA adhesin (NGO_0229) was observed in the Δ*ackA* mutant. Whole genome sequencing demonstrated differences between *pilE* alleles between the wild-type, Δ*ackA* and Δ*pta* strains with the most significant change a 80 bp deletion of the central part of the *pilE* gene of the mutants compared to the wild-type (Figure S3).

Due to the decrease in a number of potential adhesins observed in the proteomic data for both the Δ*ackA* and Δ*pta* mutant strains. Adherence of the WT and mutants was tested to the human endometrial cell line HEC-1B (Figure 8A). Both mutants had a significant reduction in adherence when compared to the WT strain, with the Δ*pta* mutant demonstrating an approximate 33% reduction in adhesion and the Δ*ackA* mutant showing an approximate 51% reduction in adherence (Figure 8A).

The greater wax moth larvae, *G. mellonella* have recently been used as an *in vivo* model for *N. gonorrhoeae* (Dijokaite et al. 2021) as it models the human innate immune response, is relatively high throughput and cost-effective. Therefore, this in vivo model was selected to test if the acetylation of proteins was involved in gonococcal pathogenesis. The pathogenicity of the three gonococcal strains were compared (Figure 8B). During the infection none of the infection-groups showed 100% survival, however, larvae infected with WT bacteria demonstrated survival of only 40% over 6 days. However, Δ*ackA* mutant infected larvae died 3 times faster than the WT and with a similar percentage of survival of 27%. While, Δ*pta* strain showed a survival percentage of 87% after 6 days post-infection that was similar to the group infected with PBS alone (Figure 8B).

4 | Discussion

In this study, the acetylome of the wild-type strain and three mutants of *N. gonorrhoeae* were investigated. The number of

20458827, 2026, 2, Downloaded from https://onlinelibrary.wiley.com/doi/10.1002/mbo3.70231 by Open Access Sheffield - UNIVERSITY OF SHEFFIELD , Wiley Online Library on [03/03/2026]. See the Terms and Conditions (https://onlinelibrary.wiley.com/terms-and-conditions) on Wiley Online Library for rules of use; OA articles are governed by the applicable Creative Commons License

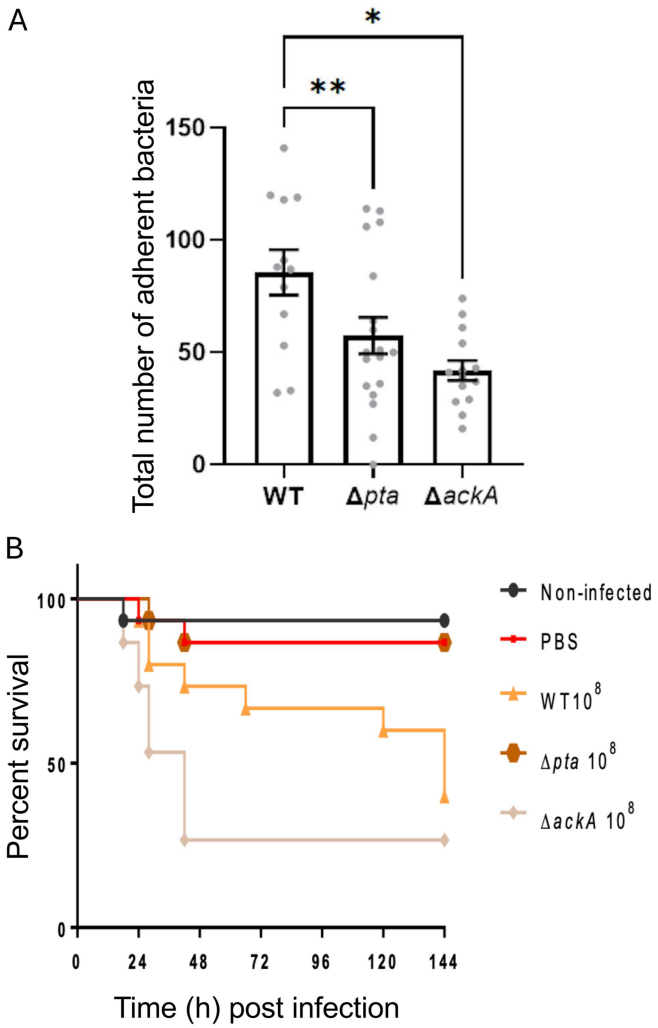

FIGURE 8 | Adherence assay of *Neisseria gonorrhoeae* to human endometrial cells and killing assay of *Galleria mellonella* infected with *N. gonorrhoeae*. (A) Adherence of *N. gonorrhoeae* strains to HEC-1B cells. The total number of bacteria adhering to the cell lines were calculated and the assays carried out on three separate occasions. The mean number of bacteria are shown with standard error. Significance was calculated using one way ANOVA with Dunnett's multiple comparison test ($p < 0.005$). (B) Survival graph showing the percentage of survival for 6 days of experiment recording results every 24 h. Groups of 20 larvae were infected each with 10 μL of different *N. gonorrhoeae* concentration. Two groups were used as controls; one injected with PBS; and one group non-infected. The larvae were infected with the WT, Δ*pta*, and Δ*ackA* strains. The group inoculated with Δ*pta* showed a higher survival than WT, similar to the control group infected with PBS. In contrast, Δ*ackA* was the strain with the lowest survival. The t-test shows a significant difference of the survival between larvae infected with Δ*ackA* and WT.

identified proteins and acetylation sites was greater than that of the previous study in *N. gonorrhoeae* (Post et al. 2017) thereby expanding the acetylome. This increased the total coverage of identified proteins increased to 55% and 40% for acetylation sites. A total of 444 proteins and 1345 acetylation sites were shared between the two studies while 327 proteins and 689 acetylation sites differed between these studies. We further add to this data by analysing Δ*pta*, Δ*ackA* and Δ*hdac* mutants. By analysing data from the most recent studies on bacterial acetylomes, that utilised immunoaffinity enrichment and mass spectrometry, we demonstrated that this study showed the highest coverage (Table S1). This was most probably due to the higher number of biological replicates, growth in CDM-GC compared to rich GC-broth and the number of strains analysed, wild type and mutants.

A number of proteins with over 20 acetylation sites with identified, including DNA-directed RNA polymerase subunit beta (RpoB), pyruvate dehydrogenase E1 component (AceE), chaperone protein ClpB (ClpB), 60 kDa chaperonin (GroEL), chaperone protein DnaK (DnaK) and DNA-directed RNA polymerase subunit beta (RpoC). Several of these proteins have been identified previously with a high number of acetylation sites (Yu et al. 2008; Kuhn et al. 2014; Post et al. 2017) and the two chaperones DnaK and GroEL have been shown to be regulated by levels of acetyl phosphate.

Enrichment analysis of the gonococcal acetylome was similar to previous bacterial studies. The highest enrichment score biological processes was for metabolic routes for pyruvate, pyrimidine and aspartate followed by translation. These first two terms were also enriched in *Salmonella* (Li et al. 2018). Whereas, in *Vibrio cholerae* translation had the highest enrichment score (Jers et al. 2018).

In this study, acetylation was shown to have an important role in the central metabolism of the *N. gonorrhoeae*. KEGG pathway analysis demonstrated numerous pathways associated with the central metabolism. Proteins involved in the TCA cycle, glycolysis, and pyruvate metabolism were identified in the acetylome of the *N. gonorrhoeae*. In other bacteria acetylation has been shown to control metabolic flux and in *S. enterica* and *Escherichia coli* acetylation of the enzymes of the central metabolism has been shown to regulate their activity (Wang et al. 2010; Zhang et al. 2013; Pisithkul et al. 2015). We observed that disrupting the PTA-AK pathway in *N. gonorrhoeae* affected the ability of the strains to grow on lactate or pyruvate but not glucose (Figure 6). We also demonstrated that a number of the enzymes involved in pyruvate metabolism are acetylated such as one of the components of pyruvate dehydrogenase E2 and phopsphotransacetylase. Furthermore, we showed that in an environment with a high intracellular concentration of acetyl-phosphate (Δ*ackA*) the specific activity of phopsphotransacetylase was reduced by 78% (Table 2). This high acetylation of enzymes involved in pyruvate metabolism maybe the reason why the Δ*ackA* strain was unable to grow on pyruvate as a sole carbon source.

Several bacterial acetylomes have shown that many of their molecular function terms were related to the binding of molecules, as was shown here (Liu et al. 2016, 2018; Jers et al. 2018). Acetylation has been shown to be involved in the regulation of gene expression through the inhibition of binding of the transcriptional regulator to their target genes (Ren et al. 2016; Koo et al. 2020).

We identified 34 unique sites with increased acetylation in the Δ*hdac* strain. Analysis of these sites demonstrated an enrichment of enzymes involved in tRNA binding suggesting that these proteins are regulated by Hdac. Similarly, in *E. coli* it was found that Ac-P acetylation of leucyl-, arginyl-, tyrosyl-, and threonyl-tRNA reduced their activity and that the deacetylase CobB that removed the acetyl group activated these tRNAs

20458827, 2026, 2, Downloaded from https://onlinelibrary.wiley.com/doi/10.1002/mbo3.70231 by Open Access Sheffield - UNIVERSITY OF SHEFFIELD, Wiley Online Library on [03/03/2026]. See the Terms and Conditions (https://onlinelibrary.wiley.com/terms-and-conditions) on Wiley Online Library for rules of use; OA articles are governed by the applicable Creative Commons License

(Ye et al. 2017; Venkat et al. 2017; Chen et al. 2019). We demonstrated an increase in acetylation in the Δ*hdac* strain of the glutamate, alanine, and valine-tRNA ligase. Other relevant proteins that were suggested to be deacetylated by Hdac were phosphotransacetylase (PTA), 2-oxoglutarate dehydrogenase, and biotin carboxylase, enzymes involved in acetyl-CoA metabolism, tricarboxylic acid cycle (TCA) and the PTA-AK pathway. The CobB deacetylase was shown to positively regulate Isocitrate lyase in *Mycobacterium tuberculosis* (Bi et al. 2017). Furthermore, in *E. coli*, enzymes of the TCA cycle, isocitrate dehydrogenase and malate dehydrogenase were shown to have an increase of activity when deacetylated by CobB (Venkat et al. 2017, 2018). The gonococcal phosphotransacetylase (Pta), the enzyme that produces acetyl-phosphate, showed an increase of acetylation of K450 in the isogenic strain Δ*hdac*. As this modification is found within the active site of the protein and we observed a PTA activity reduction within the Δ*ackA* mutant this suggests that acetylation/deacetylation maybe a way to modulate PTA activity and direct carbon flux in *N. gonorrhoeae*.

The type IV pili of *N. gonorrhoeae* are important virulence determinants that help with the colonisation of the host. Within the mutant strains generated in this study, we found differences in pili-related protein expression. The levels of PilE and PilC were found to significantly increase and decrease in Δ*ackA* and Δ*pta*, respectively. Both have been demonstrated to be important for pilus biogenesis and epithelial adherence which could explain the observed differences in gonococcal virulence (Rudel et al. 1992; Rotman et al. 2016). However, these proteins are subject to antigenic and phase variation, respectively (Swanson et al. 1987; Green et al. 2019), which may vary expression between our replicates. Indeed, whole genome sequencing of the revealed differences in the *pilE* nucleotide sequence between the wild-type and mutants resulting in different antigenic variants that could explain the observations. However, there are several non-variable pilus-associated proteins that are also affected in our study, including PilP, which showed a significant increase in acetylation in the Δ*ackA* strain. This could alter pilin biogenesis and therefore decrease adherence and invasion compared to the Δ*pta* mutant. Previous studies have shown that acetylation of PilT can change the viability of *N. gonorrhoeae* (Hockenberry et al. 2018). We did not observe any differences in PilT between strains. When assayed for adherence we observed a reduction in adherence for both the Δ*ackA* and Δ*pta* mutants versus the wild-type.

We investigated the role of the PTA-AK pathway in *N. gonorrhoeae* pathogenesis utilising the recently published gonococcal infection model for *G. mellonella* (Dijokaite et al. 2021). The gonococcal Δ*ackA* mutant killed faster than the WT and with a similar survival percentage, while the Δ*pta* resulted in a ≈90% survival. Interestingly, mice infected with a *S. enterica* Typhimurium Pta mutant showed a significantly longer survival compared to a WT strain (Kim et al. 2006), further suggesting that Ac-P or acetylation can drive bacterial virulence. A study with *E. coli* mutated in the two-component system (TCS) Cpx envelope stress regulator (CpxR) demonstrated a loss of lethality in *G. mellonella* (Leuko and Raivio 2012). In the *N. gonorrhoeae* MisRS are homologues of the Cpx system (Mitrophanov and Groisman 2008). MisRS are involved in the regulation of gonococcal virulence factor expression and have been associated with resistance to cationic antimicrobial peptides and some antibiotics (Kandler et al. 2016). In agreement with the study of Post et al. (2017) we also observed an increase in acetylation of MisR in the Δ*ackA* mutant. A putative control of MisRS by acetyl-phosphate coupled with changes in gonococcal virulence within a *Galleria* larval killing assay dependent on acetylation state suggest an intriguing link between these two pathways.

In this study, we have shown that 88% of the detectable gonococcal proteome is acetylated. Many of these acetylated proteins are involved in central metabolism and pyruvate utilisation including phosphotransacetylase. Changes in the acetylation state affected the ability to utilise particular carbon sources, especially pyruvate. We demonstrated that the enzymes of PTA-AK pathway are important for gonococcal adherence and survival in the wax moth model. Therefore, protein acetylation in *N. gonorrhoeae* plays an important role in carbon source utilisation, central metabolism, and pathogenicity.

Author Contributions

Ernesto F. D. Parga: conceptualization, methodology, investigation, formal analysis. **Paige A. Wolverson:** investigation, formal analysis. **Mark O. Collins:** investigation, formal analysis. **Oliver Heaney:** investigation, formal analysis. **Joby Cole:** investigation, formal analysis. **Luke R. Green:** conceptualization, supervision, formal analysis, writing – original draft, writing – review and editing. **Jonathan G. Shaw:** conceptualization, funding acquisition, supervision, formal analysis, writing – original draft, writing – review and editing.

Acknowledgments

E.F.D.P. was supported by a PhD student ship from CONACyT and the University of Sheffield.

Ethics Statement

The authors have nothing to report.

Conflicts of Interest

The authors declare no conflicts of interest.

Data Availability Statement

The mass spectrometry data have been deposited in the ProteomeXchange Consortium via the PRIDE partner repository with the dataset identifier (PXD060162).

References

Note: References which are denoted by * are cited in Supplementary Table 3.

Bi, J., Y. Wang, H. Yu, et al. 2017. "Modulation of Central Carbon Metabolism by Acetylation of Isocitrate Lyase in *Mycobacterium tuberculosis*." *Scientific Reports* 7: 44826. https://doi.org/10.1038/srep44826.

Catenazzi, M. C. E., H. Jones, I. Wallace, et al. 2014. "A Large Genomic Island Allows *Neisseria meningitidis* to Utilize Propionic Acid, With Implications for Colonization of the Human Nasopharynx." *Molecular Microbiology* 93: 346–355. https://doi.org/10.1111/mmi.12664.

Chen, H., S. Venkat, D. Hudson, T. Wang, Q. Gan, and C. Fan. 2019. "Site-Specifically Studying Lysine Acetylation of Aminoacyl-tRNA Synthetases." *ACS Chemical Biology* 14: 288–295. https://doi.org/10.1021/acschembio.8b01013.

20458827, 2026, 2, Downloaded from https://onlinelibrary.wiley.com/doi/10.1002/mbo3.70231 by Open Access Sheffield - UNIVERSITY OF SHEFFIELD , Wiley Online Library on [03/03/2026]. See the Terms and Conditions (https://onlinelibrary.wiley.com/terms-and-conditions) on Wiley Online Library for rules of use; OA articles are governed by the applicable Creative Commons License

Dijokaite, A., M. V. Humbert, E. Borkowski, R. M. La Ragione, and M. Christodoulides. 2021. "Establishing an Invertebrate *Galleria mellonella* Greater Wax Moth Larval Model of *Neisseria gonorrhoeae* Infection." *Virulence* 12: 1900–1920. https://doi.org/10.1080/21505594.2021.1950269.

Dillard, J. P. 2011. "Genetic Manipulation of *Neisseria gonorrhoeae*." *Current Protocols in Microbiology* 23: Unit4A.2. https://doi.org/10.1002/9780471729259.mc04a02s23.

English, D. M., S. N. Lee, K. A. Sabat, et al. 2024. "Rapid Degradation of Histone Deacetylase 1 (HDAC1) Reveals Essential Roles in Both Gene Repression and Active Transcription." *Nucleic Acids Res gkae* 1223: gkae1223. https://doi.org/10.1093/nar/gkae1223.

Exley, R., L. Goodwin, Y. Li, et al. 2005. "The *Neisseria meningitidis* Lactate Permease Is Required for Nasopharyngeal Colonisation." *Infection and Immunity* 73: 5762–5766. https://doi.org/10.1128/IAI.73.9.5762-5766.2005.

Exley, R., J. G. Shaw, E. Mowe, et al. 2005. "Available Carbon Source Influences the Resistance of *Neisseria meningitidis* Against Complement." *Journal of Experimental Medicine* 201: 1637–1645. https://doi.org/10.1084/jem.20041548.

Exley, R. M., H. Wu, J. Shaw, et al. 2007. "Lactate Acquisition Promotes Successful Colonization of the Murine Genital Tract by *Neisseria gonorrhoeae*." *Infection and Immunity* 75: 1318–1324. https://doi.org/10.1128/IAI.01530-06.

Felix Diaz Parga, E. 2021. The Role of Acetyl-Phosphate in the Pathogenesis of Neisseria Gonorrhoeae MS11. PhD Thesis oai:etheses.whiterose.ac.uk:29006.

Fifer, H., J. Saunders, S. Soni, S. T. Sadiq, and M. FitzGerald. 2020. "2018 UK National Guideline for the Management of Infection With *Neisseria gonorrhoeae*." *International Journal of STD & AIDS* 31: 4–15. https://doi.org/10.1177/0956462419886775.

Grabiec, A. M., and J. Potempa. 2018. "Epigenetic Regulation in Bacterial Infections: Targeting Histone Deacetylases." *Critical Reviews in Microbiology* 44: 336–350. https://doi.org/10.1080/1040841X.2017.1373063.

Green, L. R., J. Cole, E. F. D. Parga, and J. G. Shaw. 2022. "*Neisseria gonorrhoeae* Physiology and Pathogenesis." *Advances in Microbial Physiology* 80: 35–83. https://doi.org/10.1016/bs.ampbs.2022.01.002.

Green, L. R., N. Dave, A. B. Adewoye, et al. 2019. "Potentiation of Phase Variation in Multiple Outer-Membrane Proteins During Spread of the Hyperinvasive *Neisseria meningitidis* Serogroup W ST-11 Lineage." *Journal of Infectious Diseases* 220: 1109–1117. https://doi.org/10.1093/infdis/jiz275.

Green, L. R., R. Issa, F. Albaldi, et al. 2023. "CD9 Co-Operation With syndecan-1 Is Required for a Major Staphylococcal Adhesion Pathway." *mBio* 14, no. 4: e0148223. https://doi.org/10.1128/mbio.01482-23.

Hockenberry, A. M., D. M. B. Post, K. A. Rhodes, M. Apicella, and M. So. 2018. "Perturbing the Acetylation Status of the Type IV Pilus Retraction Motor, PilT, Reduces *Neisseria gonorrhoeae* Viability." *Molecular Microbiology* 110: 677–688. https://doi.org/10.1111/mmi.13979.

Huang, D. W., B. T. Sherman, Q. Tan, et al. 2007. "DAVID Bioinformatics Resources: Expanded Annotation Database and Novel Algorithms to Better Extract Biology From Large Gene Lists." *Nucleic Acids Research* 35: W169–W175. https://doi.org/10.1093/nar/gkm415.

Jers, C., V. Ravikumar, M. Lezyk, et al. 2018. "The Global Acetylome of the Human Pathogen *Vibrio cholerae* V52 Reveals Lysine Acetylation of Major Transcriptional Regulators." *Frontiers in Cellular and Infection Microbiology* 7: 1–13. https://doi.org/10.3389/fcimb.2017.00537.

Jiang, Q., W. Chen, Y. Qin, et al. 2017. "AcuC, a Histone Deacetylase, Contributes to the Pathogenicity of *Aeromonas hydrophila*." *MicrobiologyOpen* 6: 1–12. https://doi.org/10.1002/mbo3.468.

Kandler, J. L., C. L. Holley, J. L. Reimche, et al. 2016. "The MisR Response Regulator Is Necessary for Intrinsic Cationic Antimicrobial Peptide and Aminoglycoside Resistance in *Neisseria gonorrhoeae*." *Antimicrobial Agents and Chemotherapy* 60: 4690–4700. https://doi.org/10.1128/AAC.00823-16.

Kim, Y. R., S. R. Brinsmade, Z. Yang, J. Escalante-Semerena, and J. Fierer. 2006. "Mutation of Phosphotransacetylase but Not Isocitrate Lyase Reduces the Virulence of *Salmonella enterica* Serovar typhimurium in Mice." *Infection and Immunity* 74: 2498–2502. https://doi.org/10.1128/IAI.74.4.2498-2502.2006.

Klein, A. H., A. Shulla, S. A. Reimann, D. H. Keating, and A. J. Wolfe. 2007. "The Intracellular Concentration of Acetyl Phosphate in *Escherichia coli* Is Sufficient for Direct Phosphorylation of Two-Component Response Regulators." *Journal of Bacteriology* 189: 5574–5581. https://doi.org/10.1128/JB.00564-07.

Koo, H., S. Park, M.-K. Kwak, and J.-S. Lee. 2020. "Regulation of Gene Expression by Protein Lysine Acetylation in Salmonella." *Journal of Microbiology* 58: 979–987. https://doi.org/10.1007/s12275-020-0483-8.

*Kosono, S., M. Tamura, S. Suzuki, et al. 2015. "Changes in the Acetylome and Succinylome of *Bacillus subtilis* in Response to Carbon Source." *PLoS One* 10: e0131169. https://doi.org/10.1371/journal.pone.0131169.

Kuhn, M. L., B. Zemaitaitis, L. I. Hu, et al. 2014. "Structural, Kinetic and Proteomic Characterization of Acetyl Phosphate-Dependent Bacterial Protein Acetylation." *PLoS One* 9: e94816. https://doi.org/10.1371/journal.pone.0094816.

Leighton, M. P., D. J. Kelly, M. P. Williamson, and J. G. Shaw. 2001. "An NMR and Enzyme Study of the Carbon Metabolism of *Neisseria meningitidis*." *Microbiology* 147: 1473–1482. https://doi.org/10.1099/00221287-147-6-1473.

Leuko, S., and T. L. Raivio. 2012. "Mutations That Impact the Enteropathogenic *Escherichia coli* Cpx Envelope Stress Response Attenuate Virulence in *Galleria mellonella*." *Infection and Immunity* 80, no. 9: 3077–3085. https://doi.org/10.1128/IAI.00081-12.

Li, L., W. Wang, R. Zhang, et al. 2018. "First Acetyl-Proteome Profiling of *Salmonella typhimurium* Revealed Involvement of Lysine Acetylation in Drug Resistance." *Veterinary Microbiology* 226: 1–8. https://doi.org/10.1016/j.vetmic.2018.09.024.

*Li, Y., H. Xue, D. Bian, G. Xu, and C. Piao. 2020. "Acetylome Analysis of Lysine Acetylation in the Plant Pathogenic Bacterium *Brenneria nigrifluens*." *MicrobiologyOpen* 9: 1–11. https://doi.org/10.1002/mbo3.952.

Liu, L., G. Wang, L. Song, B. Lv, and W. Liang. 2016. "Acetylome Analysis Reveals the Involvement of Lysine Acetylation in Biosynthesis of Antibiotics in Bacillus Amyloliquefaciens." *Scientific Reports* 6: 20108. https://doi.org/10.1038/srep20108.

Liu, Y.-T., Y. Pan, F. Lai, et al. 2018. "Comprehensive Analysis of the Lysine Acetylome and Its Potential Regulatory Roles in the Virulence of *Streptococcus pneumoniae*." *Journal of Proteomics* 176: 46–55. https://doi.org/10.1016/j.jprot.2018.01.014.

McCleary, W. R., J. B. Stock, and A. J. Ninfa. 1993. "Is Acetyl Phosphate a Global Signal In *Escherichia coli*?" *Journal of Bacteriology* 175: 2793–2798. https://doi.org/10.1128/jb.175.10.2798.1993.

Mitrophanov, A. Y., and E. A. Groisman. 2008. "Signal Integration in Bacterial Two-Component Regulatory Systems." *Genes & Development* 22: 2601–2611. https://doi.org/10.1101/gad.1700308.

Morse, S. A., and L. Bartenstein. 1980. "Purine Metabolism in *Neisseria gonorrhoeae*: The Requirement for Hypoxanthine." *Canadian Journal of Microbiology* 26: 13–20. https://doi.org/10.1139/m80-003.

Olsen, J. V., B. Blagoev, F. Gnad, et al. 2006. "Global, In Vivo, and Site-Specific Phosphorylation Dynamics in Signaling Networks." *Cell* 127: 635–648. https://doi.org/10.1016/j.cell.2006.09.026.

20458827, 2026, 2, Downloaded from https://onlinelibrary.wiley.com/doi/10.1002/mbo3.70231 by Open Access Sheffield - UNIVERSITY OF SHEFFIELD , Wiley Online Library on [03/03/2026]. See the Terms and Conditions (https://onlinelibrary.wiley.com/terms-and-conditions) on Wiley Online Library for rules of use; OA articles are governed by the applicable Creative Commons License

*Pang, H., W. Li, W. Zhang, et al. 2020. "Acetylome Profiling of Vibrio Alginolyticus Reveals Its Role in Bacterial Virulence." *Journal of Proteomics* 211: 103543. https://doi.org/10.1016/j.jprot.2019.103543.

Parsons, N. J., J.-P. Emond, M. Goldner, et al. 1996. "Lactate Enhancement of Sialylation of Gonococcal Lipopolysaccharide and of Induction of Serum Resistance by CMP-NANA Is Not Due to Direct Activation of the Sialyltransferase: Metabolic Events Are Involved." *Microbial Pathogenesis* 21: 193–204. https://doi.org/10.1006/mpat.1996.0054.

Pisithkul, T., N. M. Patel, and D. Amador-Noguez. 2015. "Post-Translational Modifications as Key Regulators of Bacterial Metabolic Fluxes." *Current Opinion in Microbiology* 24: 29–37. https://doi.org/10.1016/j.mib.2014.12.006.

Post, D. M. B., B. Schilling, L. M. Reinders, et al. 2017. "Identification and Characterization of AckA-Dependent Protein Acetylation in *Neisseria gonorrhoeae*." *PLoS One* 12: e0179621. https://doi.org/10.1371/journal.pone.0179621.

Public Health England. 2018. "Sexually Transmitted Infections and Screening for Chlamydia in England." *HPR* 12: 20.

Ren, J., Y. Sang, Y. Tan, et al. 2016. "Acetylation of Lysine 201 Inhibits the DNA-Binding Ability of PhoP to Regulate Salmonella Virulence." *PLoS Pathogens* 12: e1005458. https://doi.org/10.1371/journal.ppat.1005458.

Rotman, E., D. M. Webber, and H. S. Seifert. 2016. "Analyzing *Neisseria gonorrhoeae* Pilin Antigenic Variation Using 454 Sequencing Technology." *Journal of Bacteriology* 198: 2470–2482. https://doi.org/10.1128/jb.00330-16.

Rudel, T., J. P. M. van Putten, C. P. Gibbs, R. Haas, and T. F. Meyer. 1992. "Interaction of Two Variable Proteins (PilE and PilC) Required for Pilus-Mediated Adherence of *Neisseria gonorrhoeae* to Human Epithelial Cells." *Molecular Microbiology* 6: 3439–3450. https://doi.org/10.1111/j.1365-2958.1992.tb02211.x.

*Schilling, B., N. Basisty, D. G. Christensen, et al. 2019. "Global Lysine Acetylation in *Escherichia coli* Results From Growth Conditions That Favor Acetate Fermentation." *Journal of Bacteriology* 201: 1–9. https://doi.org/10.1128/jb.00768-18.

Swanson, J. 1972. "Studies on Gonococcus Infection." *Journal of Experimental Medicine* 136: 1258–1271. https://doi.org/10.1084/jem.136.5.1258.

Swanson, J., K. Robbins, O. Barrera, et al. 1987. "Gonococcal pilin Variants in Experimental Gonorrhea." *Journal of Experimental Medicine* 165: 1344–1357. https://doi.org/10.1084/jem.165.5.1344.

UK Health Security Agency. 2023. "GRASP Report: Data to June 2023 [Internet]." https://www.gov.uk/government/publications/gonococcal-resistance-to-antimicrobials-surveillance-programme-grasp-report/grasp-report-data-to-june-2023#main-findings.

Unemo, M., M. M. Lahra, M. Cole, et al. 2019. "World Health Organization Global Gonococcal Antimicrobial Surveillance Program (WHO GASP): Review of New Data and Evidence to Inform International Collaborative Actions and Research Efforts." *Sexual Health* 16: 412–425. https://doi.org/10.1071/SH19023.

Venkat, S., H. Chen, A. Stahman, et al. 2018. "Characterizing Lysine Acetylation of Isocitrate Dehydrogenase in *Escherichia coli*." *Journal of Molecular Biology* 430: 1901–1911. https://doi.org/10.1016/j.jmb.2018.04.031.

Venkat, S., C. Gregory, Q. Gan, and C. Fan. 2017. "Biochemical Characterization of the Lysine Acetylation of Tyrosyl-tRNA Synthetase in *Escherichia coli*." *ChemBioChem* 18: 1928–1934. https://doi.org/10.1002/cbic.201700343.

Venkat, S., C. Gregory, J. Sturges, Q. Gan, and C. Fan. 2017. "Studying the Lysine Acetylation of Malate Dehydrogenase." *Journal of Molecular Biology* 429: 1396–1405. https://doi.org/10.1016/j.jmb.2017.03.027.

Verdin, E., and M. Ott. 2013. "Acetylphosphate: A Novel Link Between Lysine Acetylation and Intermediary Metabolism in Bacteria." *Molecular Cell* 51: 132–134. https://doi.org/10.1016/j.molcel.2013.07.006.

Wand, M. E., C. M. Müller, R. W. Titball, and S. L. Michell. 2011. "Macrophage and *Galleria mellonella* Infection Models Reflect the Virulence of Naturally Occurring Isolates of *B. pseudomallei*, *B. thailandensis* and *B. oklahomensis*." *BMC Microbiology* 11: 11. https://doi.org/10.1186/1471-2180-11-11.

Wang, Q., Y. Zhang, C. Yang, et al. 2010. "Acetylation of Metabolic Enzymes Coordinates Carbon Source Utilization and Metabolic Flux." *Science* 327: 1004–1007. https://doi.org/10.1126/science.1179687.

Weinert, B. T., V. Iesmantavicius, S. A. Wagner, et al. 2013. "Acetyl-Phosphate Is a Critical Determinant of Lysine Acetylation in *E. coli*." *Molecular Cell* 51: 265–272. https://doi.org/10.1016/j.molcel.2013.06.003.

Wolfe, A. J. 2016. "Bacterial Protein Acetylation: New Discoveries Unanswered Questions." *Current Genetics* 62: 335–341. https://doi.org/10.1007/s00294-015-0552-4.

*Xu, J.-Y., Z. Xu, X. Liu, M. Tan, and B.-C. Ye. 2018. "Protein Acetylation and Butyrylation Regulate the Phenotype and Metabolic Shifts of the Endospore-Forming *Clostridium acetobutylicum*." *Molecular & Cellular Proteomics* 17: 1156–1169. https://doi.org/10.1074/mcp.RA117.000372.

Yu, B. J., J. A. Kim, J. H. Moon, S. E. Ryu, and J.-G. Pan. 2008. "The Diversity of Lysine-Acetylated Proteins in *Escherichia coli*." *Journal of Microbiology and Biotechnology* 18: 1529–1536.

Zhang, K., S. Zheng, J. S. Yang, Y. Chen, and Z. Cheng. 2013. "Comprehensive Profiling of Protein Lysine Acetylation in *Escherichia coli*." *Journal of Proteome Research* 12: 844–851. https://doi.org/10.1021/pr300912q.

Zughaier, S. M., C. E. Rouquette-Loughlin, and W. M. Shafer. 2020. "Identification of a *Neisseria gonorrhoeae* Histone Deacetylase: Epigenetic Impact on Host Gene Expression." *Pathogens* 9, no. 2: 132. https://doi.org/10.3390/pathogens90.

Supporting Information

Additional supporting information can be found online in the Supporting Information section.

Supplemental Figure 1: Gene ontology enrichment analysis of N. gonorrhoeae MS11 acetylome. **Supplemental Figure 2:** Correlation of CFE for sample validation. **Supplemental Figure 3:** Alignment of the nucleotide sequence region of *pilE*. **Supplementary Table 1:** Maxquant proteinGroups output and Perseus statistical analysis output for the proteomic analysis of ackA, pta and, hdac mutant strains compared to WT. Peptide/protein identifications have been filtered to an FDR of 1% and reverse and contaminant hits have been removed. Statistical analysis of the quantitative data was performed uisng *t*-testing with a permutation-based FDR 0.05. Imputed Intensities are highlighted in yellow. **Supplementary Table 2:** Maxquant proteinGroups output and Perseus statistical analysis output for the proteomic analysis of ackA, pta and, hdac mutant strains compared to WT. Peptide/protein identifications have been filtered to an FDR of 1% and reverse and contaminant hits have been removed. Class I acetylation sites were defined by a localization probability of > 0.75 and a score diff > 5. Statistical analysis of the quantitative data was performed uisng *t*-testing with a permutation-based FDR 0.05. Imputed Intensities are highlighted in yellow. **Supplemental Table 3:** Comparison of studies with bacterial acetylomes.

20458827, 2026, 2, Downloaded from https://onlinelibrary.wiley.com/doi/10.1002/mbo3.70231 by Open Access Sheffield - UNIVERSITY OF SHEFFIELD , Wiley Online Library on [03/03/2026]. See the Terms and Conditions (https://onlinelibrary.wiley.com/terms-and-conditions) on Wiley Online Library for rules of use; OA articles are governed by the applicable Creative Commons License